06.07.2015

Prof. M. van den Broeke

Revised version of paper

Dear Prof. van den Broeke,

Please, find below a detailed rebuttal letter (including a version of the paper with changed parts marked) to the very constructive critics of both reviewers. We further attach a version of the manuscript with changes marked in the colours (referring to the comments of the editors in blue and brown, as well as corrections introduced by ourselves in green). We think that we have met all the requests by the reviewers and are looking forward to receiving your comments on the revised version of the manuscript.

With kind regards on behalf of all co-authors,

Thomas Zwinger

Senior application scientist

CSC – IT Center for Science Ltd.

Response to reviews of *Interaction of katabatic wind and local surface mass balance at Scharffenbergbotnen Blue Ice Area, Antarctica*

We want to thank both reviewers for their very constructive critics. Please, find below a detailed response to the general as well as detailed remarks kept in separate colours in order to distinguish between the two reviews. We further attach a version of the manuscript with changes marked in these colours, referring to the comments of the reviewers in blue (reviewer 1) and brown (reviewer 2), as well as corrections introduced by ourselves (in green). In particular, we have been improving the post-processing, now showing vertical cross-sections as well as a (limited to a certain time-window) statistical analysis of the flow. In order to justify the assumption of incompressibility of the flow, which was the strongest concern of reviewer 2 and is a valid argument if dealing with the complete dynamics of such events, we added a dimensional analysis in the form of an appendix in order to show that for the short distances/high velocities upon impact of an approaching jet into the valley of Scharffenbergbotnen, the non-dimensional groups allow for such an assumption to be justified. We think that with applying the changes in the manuscript, we have met all the requests by the reviewers.

Reviewer #1

Review of "Interaction of katabatic wind and local surface mass balance at Scharffenbergbotnen Blue Ice Area, Antarctica" by T. Zwinger et al.

This manuscript presents the application of a direct numerical simulation to a katabatic wind event around an East Antarctic blue ice area (BIA). The results show that wind speeds are highest on the BIA, underlining the importance of katabatic wind events in effectively removing snow from the BIA. The paper also shows that the marked present-day topography, with the BIA surrounded by nunataks, is a necessary condition for the high wind speeds on the BIA.

This is an original approach of a high-resolution numerical model, to explain the existence of a high-elevation BIA in Antarctica. The subject is well suited for publication in The Cryosphere, the methods appear well described (although I am not particularly experienced in DNS setups), and the manuscript is well written. However, my overall impression is that the authors could expand on the analysis of the results; the results section is rather short compared to the methods. The authors should analyse of the vertical wind profiles on/around the BIA, analysis of the wind direction, temporal variability etc. Furthermore, I have some general and some textual comments, which hopefully assist the authors in further strengthening the paper.

We thank the reviewer for the general positive assessment of the manuscript and the suggestions and corrections proposed. Post-processing of 4D turbulent flows is a challenge, but along the suggestions of the reviewer we added a vertical cross-section that cuts through the large inner BIA (the one of interest) displaying the velocity for every output step. Doing temporal statistics on highly time-varying turbulent flows (as the impact of a jet into a valley is) is difficult. Nevertheless, we added one figure showing the average and standard deviation velocity over a time period of 100 seconds around 1000 seconds into the reference-simulation with the nose-shape profile, showing statistics at a point in time when the katabatic front has covered most of the inner BIA. The findings from this confirm that highest velocities as well as fluctuations (which can be interpreted as by the model resolved turbulence) are most prominent above the inner northern BIA.

Title: the title does not at all cover the content of the paper, as it does not analyse the interaction between wind and SMB, rather just presents the simulation of a strong katabatic wind event.
We agree that the title can be misleading, but we certainly have done more than simulate a single katabatic event.. We changed the title to: *Numerical simulations and observations of the role of katabatic winds in the creation and maintenance of Scharffenbergbotnen Blue Ice Area, Antarctica*

Abstract:
L1: We model… I would start with a more general sentence: "We simulate the near-surface wind distribution during a katabatic wind event on a blue ice…"
We disagree in the sense that the reviewers suggestion would imply that we studied just a single event. We did far more than that. We examined the role of wind and surface topography and ice sheet elevations on the BIA within SBB which is not a single modelling exercise. In order to be sure that the opening sentence gives the correct impression of what we did in the paper, we changed to the following formulation: *We model the role of katabatic winds in the formation and maintenance of a blue ice area in Scharffenbergbotnen valley, Antarctica using the finite element code Elmer*.

L2: high-resolution (50-200 m)
We changed to: *high horizontal resolution (50 – 200 m)*

L5: enhanced wind-impact = high wind speeds
With wind-impact we wanted to emphasize the near-surface location of these strong winds. We stick to a similar formulation as suggested by the reviewer and changed the expression into: *high near-surface wind speeds*

L13: later than the = after the
Changed as suggested.

Introduction:
L20: remove "on the Antarctic… clear of snow"
Indeed, this was a strange sentence. We changed into: *A Blue Ice Area (BIA) is a snow-free ablation zone where the surface ice reflects a blueish color.*

L23: are sufficiently high to
Changed, as suggested.

P2233, L1: occur, not even in summer, Perhaps other examples of DNS solutions of katabatic winds should be added here, see e.g. Axelsen and Van Dop, 2009.
We included this example of a LES investigation in the references.

Section 2:
Does the model only resolve wind speed, or also other atmospheric variables? Give a broader introduction of the DNS methodology and its relevance for cryospheric research.
We do not really see DNS (Direct Numerical Simulation – as we interpret it) being linked to the context of our simulations, as DNS – by the demands imposed by Kolmogorov's theory – is not applicable to the size of problems and range of Reynolds-numbers we are dealing with. Assuming that the reviewer wanted to include the context between VMS and the related Large Eddy Simulation (LES) method (in a wider context both can be seen as sub-grid scale methods), we added a few lines on this in Section 3.1 (former 2.1). For the first question: In the end (being not compressible, hence lacking a connection between density, pressure and temperature), the model resolves only wind speeds.

P2235, L3-5: mention units
We added a table with the corresponding physical values used in the simulations.

P2236, Equation 3: the symbols are unclear, what do they represent? Since there is no further mentioning of these in the text, I suggest removing this equation.
They represent, as indicated in the trailing text, the spaces of the FEM discretization and they re-occur in the following equation. We agree that – in view of this not being a paper that focuses on the numerical methods – we perhaps better drop this extra equation but leave the symbols in the following (earlier Eq. (4)), explaining their meaning in a sentence thereafter.

P2237,L3: At each time step,
Changed, as suggested

P2238, L8: Why is the wind introduced at the eastern boundary? Is there any observational evidence that the strongest katabatic winds are in in fact originating from the east? I miss an analysis and figures of the wind direction; along with wind speed gradients, wind direction determines the atmospheric flow divergence, ultimately controlling the drifting snow distribution.
The wind is introduced at the eastern boundary because there are clear indications that katabatic winds come from that direction, firstly, simply because the deepest gradient of the ice-sheet is aligned with this direction and, secondly (as indicated in the caption of Fig. 1), there is clear evidence provided by wind tails behind nunataks of the prevailing easterly origin of strong events at SBB.

L32: mention units. Is there any observational/theoretical evidence for the choice of these distributions?
We assume that that the reviewer is referring to the profile equations (starting at line 23 and not 32). Units have been added. We have no direct observational evidence of the inflow profile at SBB, hence we chose to use a variety (in shape as also vertical extension) of the inflow profiles to study the dependence. Motivated by another comment of this review-round we have included a more detailed discussion of the influence of the chosen inflow profile on the wind distribution.

Sections 4.2 and 4.3:
I suggest adding figures showing vertical profiles of wind speed for the different sensitivity runs. Perhaps it might be interesting to spatially average the wind speeds for the BIAs to see the overall effect of changing the topography. Moreover, the spatial figures and animated gifs are useful, but I would suggest enlarging the figures and marking the location of the BIA more clearly.
We added vertical cross-sections to the already existing horizontal ones. We also improved the visibility of the BIAs. Furthermore we added one additional figure showing the averaged velocities and the standard deviation (which can be interpreted as a measure for the large scale turbulence) for a time window of 100 seconds around 1000 seconds into the simulation.

Section 5:
This is an interesting section, but it should be better linked to the other results; for instance, this section could be moved to the first part of the results, and be used as a motivation to study/simulate (in absence of observations) katabatic wind events.
We think that the current sections 2 and 3 about the equations and the simulation setup should not be separated by what is currently section 4. But we agree that from the structure it is advantageous to firstly present the observed katabatic event. Thereby we decided to pull that part linked to observation even before introducing the simulation setup.

Reviewer #2

Interactivecommenton"Interaction of katabatic wind and local surfacemassbalance at Scharffenbergbotnen Blue Ice Area,Antarctica" by T.Zwinger et al.

Dear Editor,

Here is my review of the manuscript entitled "Interaction of katabatic wind and local surface mass balance at Scharffenbergbotnen Blue Ice Area, Antarctica." General remarks: The manuscript uses finite element code Elmer to model the winds that cause the formation of blue ice area (BIA) in Scharffenbergbotnen valley, Antarctica. The authors use incompressible Navier-Stokes equation, and with boundary conditions (as I understand it) to resemble katabatic flow. This is a high resolution model with 50 m horizontal resolution inside the valley where the BIAs are located. Three variations of vertical wind velocity profile of the katabatic wind front are used here. Katabatic winds follow the ice surface topography and therefore the experiment setup is to understand the affect of topography on the formation of BIA. Of the three types of terrains used, the authors find that the present day topography constructed from a DEM derived from airborne survey is capable of producing the high wind speeds at the locations of BIAs. A smoother topography as well as a prescribed ice surface elevation for the LGM fails to produce the high winds that would be required if the observed BIA was to exist leading to the conclusion that the BIA in this valley is younger than the LGM. In the end, the authors describe an actual katabatic storm that develops in the region of the BIA when the atmosphere is calm and stable elsewhere. The authors note a 30% increase in BIA during this time. On the other hand, a synoptic storm that produces high wind speeds in the surrounding region on some other day does not affect the BIA region at all leading the authors to believe that the BIA in the Scharffenbergbotnen valley is maintained by individual katabatic storms not by strong synoptic events.
This work is significant because it involves a high resolution model to simulate katabatic winds that lead to the formation of blue ice areas in Antarctica and has the potential of extending it to other places in Antarctica where katabatic winds routinely scour the ice surface. The manuscript is generally well written and the work is very interesting. My main problem with it is that I got stuck while trying to understand how an incompressible Navier-Stokes equation could be used to simulate katabatic winds that inherently require a variable density. The results, however, are very convincing and that intrigued me. I think I found the answer in the boundary conditions they use, but the authors need to make this clear earlier in the manuscript. I support publication after the comments are addressed.
The abstract needs a little reordering of the sentences. The figures need some tweaking to bring out the details.

We thank the reviewer for this encouraging statement and the detailed suggestions.
With respect to the strongest concern on whether an incompressible model is capable of simulating a katabatic event we argue as follows: if looking on the complete scale (starting with the formation of the event) the concern of the reviewer is indeed valid. It would not be possible to simulate a katabatic event from its very beginning in the interior of the ice-sheet using incompressible Navier-Stokes. We explicitly state this in the new version of the paper. But – and we added this line of arguments in form of a dimensional analysis in the Appendix of the new version of the paper – it is sufficient if we investigate the last few hundred metres of the whole katabatic event and the impact of the incoming jet.

To summarize the arguments presented in the Appendix: if we use the Boussinesq approximation (i.e., density differences only occurring in the term of the driving-force) and non-dimensionalize the equations (here already splitting of the hydrostatic part of the pressure), we end up with

$$\frac{\partial \boldsymbol{u}^*}{\partial t^*} + (\boldsymbol{u}^* \cdot \nabla^*)\boldsymbol{u}^* + \nabla^* p^* - \mathrm{Re}^{-1} 2\mathbf{div}^*(\bar{\bar{\varepsilon}}^*(\boldsymbol{u}^*)) = -\frac{\mathrm{Gr}}{\mathrm{Re}^2}\boldsymbol{e}_z ,$$

with the acceleration terms, the pressure gradient and the (vanishingly small) viscous contributions on the left-hand side and the contribution by density differences on the right-hand side. If we insert the characteristic values used in our simulation, we obtain the following order-of-magnitude values

$$\mathrm{Re}^{-1} = \frac{\mu}{\rho U L} = \mathcal{O}(10^{-10}) , \quad \frac{\mathrm{Gr}}{\mathrm{Re}^2} = \beta \Delta T g L U^{-2} = \mathcal{O}(10^{-2}) .$$

The symbols *U*, *L* and ΔT stand for the characteristic velocity, length-scale and temperature difference, whereas β denotes the linear thermal expansion coefficient of air, g the acceleration due to gravity and μ is the viscosity. The extremely small value of the inverse of the Reynolds-number (left) gives the scale for viscous in relation to inertia forces and indicates the turbulent nature of the flow, the second non-dimensional group represents the ratio between buoyancy and inertia, indicating that the latter dominates at these length-scales (it admittedly does not at longer length scales and/or smaller velocities).

My specific comments are below:

P 2232 L4: show highly spatially variable . . . sounds weird. suggestion: High spatial variability in wind . . .
Changed, as suggested.

P 2232 L6: I think this line should appear later in the abstract at L 16.
We moved this now slightly altered (in order to rebuild the context to the present day topography) sentence to a later position in the abstract.

P2232 L13: Is located further interior in the valley. . .?
we simplified to: ... *formation of the inner blue ice area* of Scharffenbergbotnen valley

P 2232 L20-21: The second part of the sentence has some redundancy. Ice surface clear of snow is the same as snow –free earlier in the sentence. You can write glacier ice is exposed and therefore reflects a bluish color.
This sentence was criticized also by the other reviewer and hence changed into something we think is also along the lines of your suggestion

P 2232 L25: compared to 'snow covered surfaces'
Changed to: *compared with snow covered surfaces*

P 2233: L6: 'must' play a role. I am trying to tighten words so it is easier to read.
Tightened, as suggested

P 2233 L19: I need arrows for wind direction.
We annotated Fig 1. with the main wind direction and the northern direction.

L2235 L1-10: I need more explanation here for those of us who do not deal with Navier-Stokes equation on a day-to-day basis. As you are using the condition of incompressibility, density is constant right? I do not understand which terms then satisfy the characteristics of katabatic winds

that form in buoyant atmosphere where the density has to change, even if small? What makes this equation simulate a katabatic wind?
I probably missed something, and that is why you need to make it clear. I agree that the results are very convincing, so it is important to understand. What exactly does the gravitational body force do in this equation?
It may be appropriate to include details in supplementary information section for interested readers.
As mentioned before, we do not claim to simulate the katabatic wind from its formation. We are rather interested in the behavior of a wall-bounded jet reaching the valley (however this jet came to exist). This seems to not have been presented in a clear way in the earlier version. By displaying and discussing the non-dimensional equations in the Appendix, we hope to shed more light on this and will of course clearly state that this approach is not valid for investigating the origins of a katabatic wind event.

P 2237 L18: I like the high horizontal resolution of 50 m in the interior.
Thanks – for that reason it is good to have a supercomputer at hand.

P2239 L6: I see the boundary conditions and see that you force the flow only along the surface and do not allow any vertical component. So essentially terrain following like a katabatic wind?
We slightly disagree, as the mesh is not terrain following (the upper boundary is at constant elevation, the bedrock not) and the height of the domain stretches way higher than the height of the close-surface jet. This is to be seen in the added vertical cross-sections. You are correct in that the upper boundary at an elevation of 3000 m does not allow for vertical velocity, as we reported in the text, nevertheless, the jet – at least in the center of the domain, where it is important - never reaches to that height. We introduced this boundary condition, as we were getting into difficulties on the southern side of the domain, where a mountain reaches quite high up and caused instabilities that were suppressed by imposing the boundary condition. The following figure shows the same setup at the phase when the jet is redirected towards the valley, once with the vertically blocked upper surface (left) and once with a complete free boundary (right). In the center domain there is no significant difference between these results.

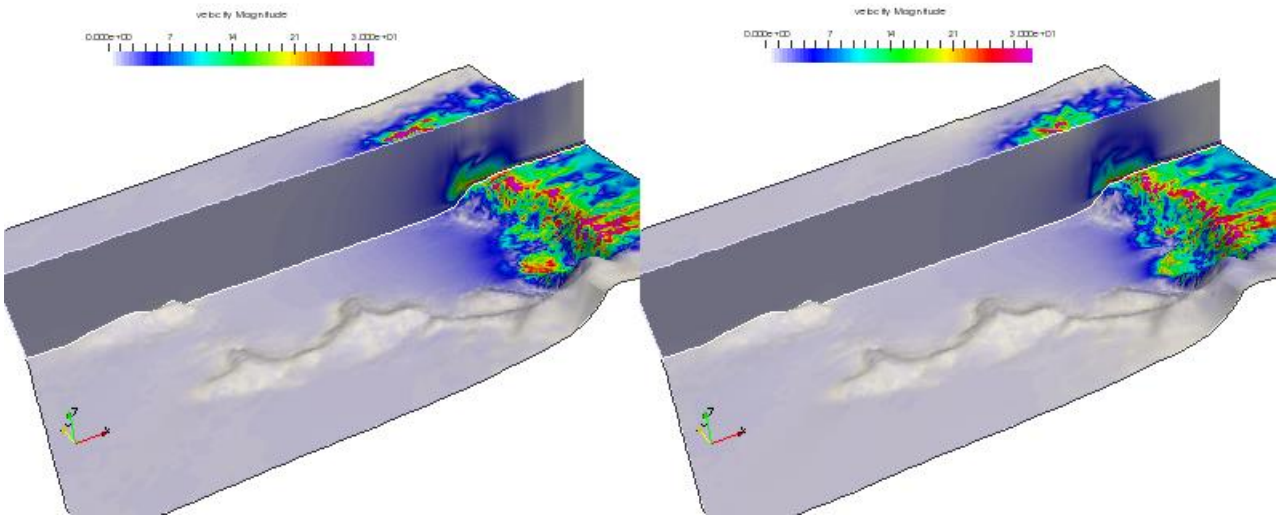

P2240: L20: This is cool!
Thanks

P2240 L22: I understand one profile will always do better than the others, but I would like to understand why the other profiles do not do as well at 5m above the ground?

One explanation could be (and we insert this into the text): *Comparing the positions of the flow-speed maxima in Fig. 6 with the results in Fig. 8 and Fig. 10 we can clearly see that the closer the maximum flow-speed of the inflow profile is to the surface, the greater the focusing of the fast flow towards the BIA seems to be. From this we conclude that the high wind speed close to the terrain creates the effect of redirection.*

P 2240 L23: In addition, what happens to these runs at 1250 s? That is when Fig 6 is most striking. Is there a reason you use 1000 s and not 1250s for the rest of the figures?
P2241, L10: Oh I think I found the answer why you use 1000 s instead of 1250 s in the other figures here.
We thereby assume that there is no demand to change the timings of write-out, as demanded for P 2240 L23

Comments on the Figures:
Please provide directions in the figures. At least show which is East, so I do not have to go back and forth between figures. An arrow for prevailing wind direction will be helpful.
We added an annotation indicating the main wind direction in Fig. 1. In Fig. 3 (formerly Fig 11) – by referring to markers in Fig 1. - we improved the description on where the destroyed camp was situated and where the debris of it was deposed and included the same markers also in Fig. 2. In all other figures we added annotations and/or markers indicating the northern direction.

Fig2: Arrows to show ice flow will be helpful here. I know they are in Zwinger et al. 2014, but the figures have to be self sufficient.
We added arrows that – supported by additional text in the caption – should give a qualitative impression on the ice dynamics inside the SBB valley. We think that adding the complete set of measured or simulated ice velocities of the 2014 article would overload the figure.

Figure 5: The equilibrium yellow and white dotted line is hard to see. Please label some of the elevation contours here and elsewhere.
We tried to enhance these features for better visibility

Fig 6: Again all the solid and dashed lines are very hard to see.
We improved the visibility of the lines indicating the BIAs and – for the sake of not overloading the figure – skipped the display of the zero accumulation line.

Please, find the revised manuscript with the applied changes kept in colours attached

Manuscript prepared for The Cryosphere Discuss.
with version 2014/09/16 7.15 Copernicus papers of the LaTeX class copernicus.cls.
Date: 6 July 2015

Numerical simulations and observations of the role of katabatic winds in the creation and maintenance of Scharffenbergbotnen Blue Ice Area, Antarctica

T. Zwinger[1,2], T. Malm[3], M. Schäfer[4], R. Stenberg[3], and J. C. Moore[2,4]

[1]CSC – IT Center for Science Ltd., P.O. Box 405, 02101 Espoo, Finland
[2]College of Global Change and Earth System Science, Beijing Normal University, 19 Xinjiekou Wai Street, Beijing, 100875 China
[3]Aalto University, Institute of Mathematics, P.O. Box 1100, 02015 HUT, Espoo, Finland
[4]Arctic Centre, University of Lapland, P.O. Box 122, 96101 Rovaniemi, Finland

Correspondence to: J. C. Moore (john.moore.bnu@gmail.com)

Abstract

We model the role of katabatic winds in the formation and maintenance of a blue ice area in Scharffenbergbotnen valley, Antarctica, using the finite element code Elmer. The high horizontal resolution (50 - 200 m) numerical simulations of the local wind flow from katabatic wind fronts show high spatial variability in wind impact patterns and good congruence between places with high near-surface wind speeds and the blue ice area. In addition we perform wind simulations on an altered glacier geometry that resembles the thicker ice cover at the Late Glacial Maximum (LGM). These simulations indicate that the pronounced spatial wind-impact patterns depend on present day geometry and did not occur during the LGM. This leads to the conclusion that the formation of the inner blue ice area of the Scharffenbergbotnen valley started only after the lowering of the ice surface, after the LGM. Experiments with smoothed surface topography suggest that detailed positions of the high wind regions and hence individual blue ice fields, may have varied as the ice sheet lowered. The simulation results obtained with the present day geometry were fortuitously confirmed by the destruction of a field camp located in a high wind speed area and its subsequent redistribution to low velocity areas. The experiments and the field observations are consistent with localized violent katabatic events, rather than synoptic scale storms, playing the dominant role in the formation and maintenance of this, and perhaps many blue ice areas.

1 Introduction

A Blue Ice Area (BIA) is a snow-free ablation zone where the surface ice reflects a blueish color. These areas cover about 1 % of the entire surface area of Antarctica (Sinisalo and Moore, 2010). At relatively low elevation BIAs, summer temperatures are sufficiently high to allow surface and internal melting, and are of great practical importance for water supply to field stations, and as landing strips for wheeled aircraft. The lower surface roughness of ice compared with snow covered surfaces allows winds to preferentially remove any freshly fallen snow from them. At higher altitudes, typically above 1000 m a.s.l. (Bintanja, 1999),

melt does not occur even in summertime, and BIAs are then maintained and created simply by the occurrence of strong winds over them. It is one of these high elevation BIAs that is object of study in this paper. The snow–ice boundaries of BIAs appear to be remarkably stable on multi-year timescales (Giaever, 1969), which indicates that repeating meteorological conditions must play a role in maintaining them (Bintanja, 1999; Sinisalo et al., 2004; Sinisalo, 2007). Old ice can often be found at the surface of some BIAs. If a good understanding of the ice dynamics were available, then the easily accessible ancient ice would be of great interest for paleoclimatic studies (Bintanja, 1999; Sinisalo et al., 2004; Moore et al., 2006; Sinisalo and Moore, 2010).

BIAs are hence typically located in areas where the local wind speed is occasionally high – either by association with mountain turbulence or in regions of strong katabatic wind flow. Here we investigate to what extent the surrounding terrain contributes to a local increase in wind-impact velocity above the well studied BIAs in the inner region of Scharffenbergbotnen (SBB) valley, Dronning Maud Land, Antarctica (located approximately at 74.56° S, 11.05° W) and compare the wind distribution patterns with the equilibrium surface mass balance distribution computed by Zwinger et al. (2014). SBB is located about 300 km inland, in the Heimefront mountain range of Dronning Maud Land (see Fig. 1). The dominant easterly wind direction can be clearly seen from the prominent wind drift tails behind exposed rocks. A geomorphological map of the SBB valley is presented in Fig. 2. The map shows three distinguishable BIAs, one on the north-western side at the entrance of the valley, and two inside the SBB valley, separated by a moraine. The two BIAs inside the valley have been the subject of various studies of meteorological (Bintanja and Reijmer, 2001), glaciological (Sinisalo and Moore, 2010) and geomorphological nature (Hättestrand and Johansen, 2005).

Numerous previous studies of winds over Antarctica have adopted simplified equations and worked on large spatial domains, ignoring small-scale details and only resolving large-scale flow patterns. A hydrostatic, three-dimensional primitive equation model with a resolution of 20 km was presented by Bromwich et al. (1994) for simulations on winter katabatic winds crossing the Siple coast and the Ross ice shelf. Gallée et al. (1994) proposed a sim-

ilar model with the highest resolution being 5 km. A relatively simple simulation of snow flow affected by katabatic winds was presented by Gallée (1998); with a horizontal resolution of 40 km, the model domain covered the entire Antarctic ice-sheet. The study by Yu et al. (2005) on katabatic jumps, where an open channel katabatic flow rapidly transforms to a calm flow was implemented on an uniform grid spacing of 3.5 km, 700 and 175 m along with an assumption of a two-dimensional katabatic flow and a rather smooth geometry. Skyllingstad (2003) in contrast used a Large Eddy Simulation (LES) to investigate the small-scale dynamics of gravity-driven incompressible flows on a simple linearly decreasing smooth slope with a resolution of approximately 0.75 m. Axelsen and van Dop (2009) applied LES to simulations of steady-state quasi-one-dimensional buoyancy-driven slope winds over glaciers.

We deploy Variational Multiscale (VMS) stabilization with the Finite Element (FE) method to study the local wind fields above the valley at SBB. To our knowledge this is the first high resolution Navier–Stokes governed simulation of local wind fields above BIAs. The domain size used for our modelling of the complex terrain in SBB is 10^3 times larger than in Skyllingstad (2003), and our minimal horizontal resolution is $h_{\text{min}} \approx 50$ m.

First we present observational evidence that the mechanism responsible for creating and maintaining the inner BIA at SBB is to be found in easterly katabatic wind fronts in Sect. 2. This provides motivation for the following analysis. In Sect. 3 we present the governing equations including a brief introduction to the VMS turbulence model in Sect. 3.1. This will be followed in Sect. 4 with a discussion of the specific model setup for the simulations of SBB area. Section 5 presents and discusses the results obtained for different flow profiles as well as altered geometries. The conclusions from these results are presented in Sect. 6.

2 Case study of observed violent wind event

In January 2007 a field camp located near the head of the Scharffenbergbotnen valley was destroyed by a strong storm (Fig. 3). There are two reasonably close Automatic Weather Stations (AWS), AWS6 and AWS9, in the region of Scharffenbergbotnen. AWS9 is located

at the summit of the regional ice field at 75°00′09″ S 00°00′26″ E and 2900 m a.s.l., while AWS6 is about 40 km north of the Scharffenbergbotnen valley at 74°28′53″ S 11°31′01″ W and 1160 m a.s.l. (Bintanja, 1999; Van den Broeke et al., 2005), the location of the weather stations in relation to Scharffenbergbotnen is shown in Fig. 1. Figure 4 shows the wind direction and magnitude recorded by the two AWSs over the first 22 days of 2007.

The largest wind speeds occur on the 11th and 12th day and are consistent in direction at the two AWS, with somewhat higher wind speeds occurring, as expected, at the lower AWS6 site. However the wind speeds in the Scharffenbergbotnen valley during the 11th and 12th day were not very high, indeed field work progressed normally on both days, with no drifting snow, and the 12th day was notably sunny and pleasant. This was a synoptic scale event that may be classed as average conditions. However the event of 2–3 January was extremely strong in Scharffenbergbotnen, but not significant on a synoptic scale, with moderate winds and inconsistent directions at AWS6 and AWS9. Such relatively stable conditions on the higher ice sheet may actually favour the formation of a katabatic jet. Even 40 km north of the Scharffenbergbotnen valley the katabatic jet had dissipated sufficiently for there to be no trace of it in the AWS6 record. The debris from the 2–3 January storm was dispersed over much of the valley and provide traces for recirculation areas. The location where the field camp was originally placed and where a tent from the destroyed camp was found is shown in Fig. 1. This and many other items were all found on snow accumulation areas and not on the blue ice area. Existing snow and even hard firn was ripped from the BIA such that the extent of the BIA was increased by perhaps 30 % relative to that before the storm. This suggests that such storms are rather infrequent, and that the BIA extent may be governed by rare stochastic events that remove the steadily accumulated snow and firn of several years. In what follows, we present a numerical model that studies the impact of a turbulent wall-bounded jet into the Scharffenberbotnen valley that enables us to identify the areas of high wind-speeds close to the ground within the valley where potentially snow can be removed.

3 Governing equations for wind flow simulations

The flow is assumed to be described by the incompressible Navier–Stokes equations

$$\rho\left(\frac{\partial \boldsymbol{u}}{\partial t}+(\boldsymbol{u}\cdot\nabla)\boldsymbol{u}\right)+\nabla p-2\mu\,\mathbf{div}(\bar{\bar{\varepsilon}}(\boldsymbol{u}))=\rho\boldsymbol{f},$$
$$\nabla\cdot\boldsymbol{u}=0, \tag{1}$$

where ρ stands for the constant density of the air, $\boldsymbol{f}$ for the gravitational body force, $\boldsymbol{u}$ denotes the velocity vector, p the isotropic pressure and μ is the dynamic viscosity . The numerical values of these parameters used in the simulation are presented in Table 1. The symmetric strain rate tensor, $\bar{\bar{\varepsilon}}$, is given by

$$\bar{\bar{\varepsilon}}(\boldsymbol{u})=\frac{1}{2}\left(\nabla\boldsymbol{u}+(\nabla\boldsymbol{u})^{\mathsf{T}}\right). \tag{2}$$

The set of Eqs. (1) and (2) is defined in the domain $\Omega\subset\mathbb{R}^3$ for the time-interval $t\in(0,t_{\text{end}})$.

We are well aware that katabatic winds are driven by the density differences between colder and warmer air and hence a detailed study would deserve a buoyant (hence compressible or at least Boussinesq-approximated) flow with its density coupled to the temperature field. Nevertheless, our study will show that over the last few hundred metres of the katabatic flow into the valley the inertia of the incoming jet is sufficient to produce wind-impact patterns that well match the observed locations of the bare ice fields in the SBB valley and hence the assumption of incompressibility is appropriate for the BIA study. In Appendix A we present equations (1) in their non-dimensional form accounting for changing density using a Boussinesq approximation. By an analysis of the non-dimensional groups we can demonstrate that in the case of a fully developed katabatic jet for the length-scales that apply in our model, the inertial forces dominate the buoancy forces, which shows the applicability of an incompressible model to this work

3.1 Variational Multiscale method

The modelling of turbulent flows is one of the most challenging areas in Mathematics and Computational Fluid Dynamics (CFD). Numerous ad hoc models to treat the turbulent nature of the resulting flow numerically have been proposed. The main idea of using these approaches is to dramatically reduce the number of nodes needed for solving turbulent CFD problems (Rautaheimo, 2001) in comparison to direct numerical solution (DNS). Sub-grid scale turbulent models, such as Large Eddy Simulation (LES) models, resolve the large scale turbulence and model the effects of sub-grid turbulence. In the case of LES the sub-grid model is obtained by spatial filtering, that imposes certain problems in particular with bounded flows.

We use the implicit Euler method for time discretization. In space, continuous piecewise isoparametric hexahedral elements are used for both the velocity and pressure. The discretization in space is a weighted least squares stabilized Galerkin method, also known under the name Variational Multi Scale (VMS) method (Hughes, 1995; Hoffman and Johnson, 2006, 2007; Bazilevs et al., 2008). The VMS-method is an alternative, yet similar method to Large Eddy Simulation (LES). The main difference between LES and VMS is that the latter projects the scales into the function spaces rather than filtering them by spatial averaging. Thus the VMS-method avoids the problems of spatial filtering, spatial differentiation in bounded domains as well as with non-constant filter widths, and the issue of choosing the correct boundary conditions for spatially averaging at large scales (John et al., 2010).

Removed former Eq. (3)

Given the initial value $\boldsymbol{u}_h^0$, the solution $(\boldsymbol{u}_h^n, p_h^n)$ for the time step $t_n = n\Delta t$, $n = 1, 2, \ldots, N$, is obtained from

$$\rho\Big(\frac{\boldsymbol{u}_h^n - \boldsymbol{u}_h^{n-1}}{\Delta t} + (\boldsymbol{u}_h^n \cdot \nabla)\boldsymbol{u}_h^n, \boldsymbol{v}\Big) + \Big(\nabla p_h^n, \boldsymbol{v}\Big) - 2\mu\Big(\bar{\bar{\epsilon}}(\boldsymbol{u}_h^n), \bar{\bar{\epsilon}}(\boldsymbol{v})\Big)$$
$$+ \sum_{\mathcal{E}} \delta_{\mathcal{E}}\Big(\rho(\boldsymbol{u}_h^n \cdot \nabla)\boldsymbol{u}_h^n + \nabla p^n, (\boldsymbol{u}_h^n \cdot \nabla)\boldsymbol{v} + \nabla q\Big)_{\mathcal{E}}$$

$$= \left(\rho \boldsymbol{f}^n, \boldsymbol{v}\right) + \sum_{\mathcal{E}} \delta_{\mathcal{E}} \left(\rho \boldsymbol{f}^n, (\boldsymbol{u}_h^n \cdot \nabla)\boldsymbol{v} + \nabla q\right)_{\mathcal{E}} \quad \forall v \in \mathcal{V}_h^0,\ \forall q \in \mathcal{W}_h, \tag{3}$$

where $(\cdot,\cdot)$ denotes the $L^2(\Omega)$-inner product and $(\cdot,\cdot)_{\mathcal{E}}$ denotes the $L^2(\mathcal{E})$-inner product for the element $\mathcal{E}$ of the mesh. $\mathcal{V}_h^0$ and $\mathcal{W}_h$ represent the finite element spaces. A constant timestep-size of $\Delta t = 0.1\,\mathrm{s}$ is applied in all simulations. The stabilization parameter is given by

$$\delta_{\mathcal{E}} = \left(\frac{1}{\Delta t} + \frac{|\boldsymbol{u}^n|}{h_{\mathcal{E}}}\right)^{-1}, \tag{4}$$

where $h_{\mathcal{E}}$ represents the size of element $\mathcal{E}$. Detailed literature on applications and the theory behind the VMS method can be found in Hughes (1995); Gravemeier (2005); Gravemeier et al. (2006); Bazilevs et al. (2008). At each time step the nonlinear system (3) is solved by a Picard iteration. The linearized system is solved using the generalized minimal residual (GMRES) Krylov-subspace method (Kelley, 1995) with an incomplete LU factorization of the system matrix deployed as a preconditioning step.

4 Simulation setup for Scharffenbergbotnen valley

The VMS method used for turbulent computations is implemented within the open source multi-physics FE-code Elmer (http://www.csc.fi/elmer). Due to a large domain size combined with a turbulent flow the problem has to be solved using High Performance Computing (HPC) on a parallel Linux cluster.

The mesh, i.e. the discretization of the domain Ω, used for computations of the wind flow inside the valley is constructed from the Digital Elevation Model (DEM) data of SBB, which has a resolution of 100 m and is based on airborne surveys in 1985/86 over the whole Heimefrontfjella area (copyright of Bundesamt für Kartographie und Geodäsie, Frankfurt am Main, http://www.bkg.bund.de). This is achieved by extruding a horizontal footprint mesh, which was created with the open source mesh generator Gmsh (Geuzaine and Remacle,

2009). A horizontal resolution of 50 m is applied inside the valley where the BIAs are located, while a characteristic mesh length of 200 m is chosen for the parts of the domain closer to the side boundaries. Thus a sufficiently fine mesh in the areas of most interest can be achieved while avoiding excessive computations. As shown in Fig. 5, this footprint mesh is vertically extruded into 30 terrain-following layers up to an elevation of 3000 m. The first 10 mesh-layers are concentrated into the lowest 10 % of the height, applying an exponential refinement of the layers towards the lower surface. Thereby a high vertical resolution (1–2 m) at the valley bottom to account for the turbulent boundary layer close to the surface is achieved. This results in a mesh with 373 620 nodes from which 358 382 (mainly hexahedral) linear bulk elements are constructed, which are bounded by 30 516 (mainly quadrilateral) linear boundary elements. This mesh is split into 64 partitions for parallel computation.

Our simulation setups resemble those from Malm (2012). However, while Malm deployed initial conditions utilizing a background wind field statistically obtained from ECWMF reanalysis data, we let the katabatic wind front impact into a region of stagnant air. No significant differences in wind-impact patterns between these background fields were found.

In addition to using present day topography, two alternative meshes were constructed: a smoothed version of the initial DEM; and one based on geomorphological evidence of the ice thickness at Late Glacial maximum (LGM) – that is a DEM with 200 m thicker ice inside and 100 m outside the valley (Näslund et al., 2000; Hättestrand and Johansen, 2005). To approximate thicker glacial ice conditions around the valley, all non-glaciated peaks outside the valley were also smoothed. The smoothing in both variants of the original DEM was achieved by replacing the elevation value of each point in the smoothed DEM by the average of all surrounding points contained within a circle of 250 m radius in the original DEM, similar to a simple moving average algorithm.

We also allow for variation in the vertical velocity profile of the katabatic wave front as it enters the eastern border of the domain. The reference simulation profile for the normal inwards pointing component of the velocity, we denote as *nose*-shaped, which is defined

with respect to the height above ground, $\mathcal{H}$ [m], as

$$u_{\text{nose}}(\mathcal{H})\,[\text{m s}^{-1}] = 2\,[\text{s}^{-1}]\,\mathcal{H} - 4\cdot 10^{-2}\,[\text{m}^{-1}\,\text{s}^{-1}]\,\mathcal{H}^2 + 2\cdot 10^{-4}\,[\text{m}^{-2}\,\text{s}^{-1}]\,\mathcal{H}^3. \quad (5)$$

The alternative is a *parabolic* profile (the same as used by Malm, 2012)

$$u_{\text{para}}(\mathcal{H})\,[\text{m s}^{-1}] = 1.2\,[\text{s}^{-1}]\,\mathcal{H} - 1.2\cdot 10^{-2}\,[\text{m}^{-1}\,\text{s}^{-1}]\,\mathcal{H}^2. \quad (6)$$

Both profiles reach from ground level to 100 m above ground. The third profile investigated is a stretched version of Eq. (5), *noseL*, which extends to 200 m above ground

$$u_{\text{noseL}}(\mathcal{H})\,[\text{m s}^{-1}] = 1.01\,[\text{s}^{-1}]\,\mathcal{H} - 1.01\cdot 10^{-2}\,[\text{m}^{-1}\,\text{s}^{-1}]\,\mathcal{H}^2 + 2.53\cdot 10^{-5}\,[\text{m}^{-2}\,\text{s}^{-1}]\,\mathcal{H}^3. \quad (7)$$

All three profiles are shown as a function of $\mathcal{H}$ in Fig. 6. To avoid issues with backflow at the lateral boundaries, the inflow profile is damped to zero 1250 m from the lateral (north and south) boundaries. Instabilities imposed by the pressure field at the start of the simulation were suppressed by allowing 100 s for the inflow profile to ramp up from resting air to peak values. On the southern and northern boundaries, which are aligned with the main flow direction, the normal component of the velocity is kept at zero. The same condition applies to the boundary with the upper atmosphere, where we constrain the vertical (z aligned) velocity component. The set of boundary conditions is completed at the valley surface, $b(x, y)$, where we impose a no-slip condition

$$\boldsymbol{u}|_{z=b} = 0, \quad (8)$$

and a further free outflow condition imposed on the western confinement. In order to avoid instabilities, any backflow at this boundary is reset to zero, i.e.,

$$\boldsymbol{u}\cdot\boldsymbol{n}\,|_{\text{west}} > 0, \quad (9)$$

where $\boldsymbol{n}$ is the outward pointing normal of the boundary.

5 Results

With the setup discussed in the previous section, we study the impact of wind on the valley. Our main focus is to study the BIA north of the moraine inside the valley, i.e., the larger one stretching from about 435 to 439 km easting and 1722.5 and 1724 km northing indicated as *inner northern BIA* in Fig. 2.

A first approach is to test the original DEM with the nose-shaped profile defined in Eq. (5) and compare it to the equilibrium surface mass balance (SMB) distribution obtained from a glacier flow model simulation (Zwinger et al., 2014) of the SBB valley, using the identical surface DEM. Assuming a non varying glacier surface, s, the equilibrium SMB is given by

$$\mathrm{SMB} = \underbrace{\frac{\partial s}{\partial t}}_{=0} + u_{\mathrm{ice}}\frac{\partial s}{\partial x} + v_{\mathrm{ice}}\frac{\partial s}{\partial y} - w_{\mathrm{ice}}, \tag{10}$$

where $(u_{\mathrm{ice}}, v_{\mathrm{ice}}, w_{\mathrm{ice}})^{\mathsf{T}}$ are the Cartesian components of the surface ice velocity vector. The SMB distribution obtained by Zwinger et al. (2014) is depicted in Fig. 7.

The sensitivity of the wind-impact distribution with respect to the inflow profile was assessed by rerunning with the slightly altered inflow conditions, as presented in Eqs. (6) and (7). We then assess the sensitivity of the solution to bottom surface topography by using the smoothed DEM. Finally, we assess the effects of the LGM topography on the wind fields.

5.1 Variations of inflow profiles

The first simulation is conducted using the nose-shaped profile given by the cubic polynomial (5). We run the simulation for slightly longer than 20 min of physical time. Figure 8 shows the velocity magnitude at 5 m above ground as well on a vertical cross-section cutting through the area above the northern inner BIA from east to west, displaying snapshots starting at 500 s (when the first gusts reach the valley bottom) in steps of 250 s to 1250 s (the end of the simulation). An animated GIF (showing steps of 50 s) of this as well as of all runs conducted can be found in the Supplement of this article. From these snapshots it is clear

that fast flow is focused on the inner BIAs. The wind speeds are consistently high above the ablation area (which largely coincides with the inner BIA) found from the glacier flow simulation, indicated by the yellow polygon in Fig. 7. In particular the close correspondence in position of the high velocity streak with the northern boundary of the larger inner BIA at 1250 s into the simulation is striking. Figure 9 shows the average as well as the standard deviation of the velocity for the time window from 950 s to 1050 s of the simulation, with peak values for both properties concentrated over the inner northern BIA. The latter can be interpreted as a measure of velocity-fluctuations on the scale of the finest mesh-size (vertically in the range of metres), which in LES represent the eddies containing the highest turbulent kinetic energy (Axelsen and van Dop, 2009).

Figure 10 shows results from similar simulations with altered inflow profiles as in Eqs. (6) and (7) at 1000 s into the simulation. Although the patterns obtained with these profiles are different from the reference run, both Fig. 10 and the supplemental animated GIFS show consistently increased velocity over the inner BIAs, confirming the phenomenon of redirected fast flow. Comparing the positions of the flow-speed maxima in Fig. 6 with the results in Fig. 8 and Fig. 10 we can clearly see that the closer the maximum flow-speed of the inflow profile is to the surface, the greater the focusing of the fast flow towards the BIA seems to be. From this we conclude that the high wind speed close to the terrain creates the effect of redirection.

5.2 Variations in the smoothness of the terrain

We are interested in how small scale topographic features may affect the flow details, and hence the impact of the DEM accuracy. To that end we smoothed the original DEM using the previously described algorithm and applied the nose-shape inflow defined by Eq. (5).The left panel in Fig. 11 (and supplementary animated GIF) shows the velocity magnitude 5 m above ground as well as on a vertical cross-section from east to west at 1000 s into the simulation. One striking difference from all runs conducted on the original terrain is that at 1000 s into the simulation the katabatic front has advanced about 1 km further into the valley. The general impression – even more supported by the series in the animated GIF than by

the single snapshot – is that the areas of high impact wind velocities are less focused on the inner BIAs, compared with the reference run (Fig. 8).

5.3 LGM simulation

The surface elevation inside the valley of SBB may have been considerably higher (Näslund et al., 2000; Hättestrand and Johansen, 2005) at the LGM. We increased the ice-thickness by a constant 200 m inside and 100 m outside the valley and smoothed the surface to resemble glaciation of present-day nunataks (i.e., ice free areas on the bounding mountains of SBB valley). The right panel in Fig. 11 shows the distribution of the velocity magnitude 5 m above ground and on a vertical cross-section from east to west. In contrast with all other simulations conducted on the present day DEM – either in its original or smoothed form – the high velocity winds in the LGM simulation are distributed more randomly over the valley and not focused over present-day BIAs. In fact, the highest velocities at 1000 s into the simulation are located at the north-western end of the valley, close to the position of the outer BIA.

6 Conclusions

By conducting local wind simulations above the Scharffenbergbotnen valley we show that katabatic surface jets coming from the east, produce high-impact wind speeds at exactly the location of the inner blue ice area. These types of wind were probably directly experienced in the field during January 2007 when a highly localized event caused clearing of surface firn, likely to be several years old, from underlying bare ice. During this event simultaneously taken direct and AWS observations support the dominant role of local katabatic events rather than synoptic storm events in formation of the Scharffenbergbotnen BIA.

Sensitivity analysis to changes in vertical wind-profile shapes and DEMs revealed that the topography is mainly responsible for the distribution of the the high wind-impact features. For all simulation runs with the present-day DEM, the derived locations of both fast wind flow and recirculation areas match well with the location of the inner BIA in the Scharffenberg-

botnen valley. In contrast, a simulation conducted with increased ice thickness imposed on the present-day DEM (resembling conditions at Late Glacial Maximium) revealed that snow and firn removal focused at the position of the inner BIA most likely occurred only after the lowering of the ice in the SBB valley. Only then did the present day shape of the surrounding rocks surface from beneath the retreating and lowering ice-sheet. In other words, the inner BIA at Scharffenbergbotnen is younger than the LGM. This is in agreement with the findings of Zwinger et al. (2014), who came to similar conclusion by looking at age/depth horizons of a full-stress ice flow model.

We suggest that other BIAs in similar mountain regimes can be effectively generated by katabatic jets, and that these jets are produced independently of synoptic storms. It is conceivable that other BIAs may be controlled by extremely powerful synoptic storms that occur from time to time and scour snow and firn from the surface of the BIAs.

Appendix A: Non-dimensional equations of motion

To evaluate the relative importance of the inertia to the buoyant forces we introduce the thermal expansion coefficient, β, in order to define the linearized density with respect to temperature, T,

$$\rho(T) = \rho_0 \left(1 - \beta \left(T - T_0\right)\right). \tag{A1}$$

Here ρ_0 is the density at the reference temperature T_0. Applying the Boussinesq approximation, i.e., inserting Eq. (A1) into the right-hand-side of the Navier-Stokes equations (1), we obtain

$$\rho_0 \left(\frac{\partial \boldsymbol{u}}{\partial t} + (\boldsymbol{u} \cdot \nabla)\boldsymbol{u}\right) + \nabla p - 2\mu\, \mathbf{div}(\bar{\bar{\varepsilon}}(\boldsymbol{u})) = -\left(1 - \beta\left(T - T_0\right)\right) \rho_0\, g\, \boldsymbol{e}_z, \tag{A2}$$

reformulating the body force, $\boldsymbol{f}$, introducing the acceleration due to gravity $\boldsymbol{f} = -g\boldsymbol{e}_z$.

If we now further introduce the typical scales for velocity, U, length, L and temperature difference, ΔT, we can express physical in terms of non-dimensional variables (indicated

with supscribed star)

$$\begin{aligned} \boldsymbol{u} &= \boldsymbol{u}^* U, & T - T_0 &= (T^* - T_0^*)\,\Delta T, \\ t &= t^* L/U, & p &= p^* \rho U^2, \\ \bar{\bar{\varepsilon}} &= \bar{\bar{\varepsilon}}^* U/L, & \boldsymbol{g} &= -g\boldsymbol{e}_z, \\ \nabla &\rightarrow L^{-1}\nabla^*, & \mathbf{div} &\rightarrow L^{-1}\mathbf{div}^*. \end{aligned} \tag{A3}$$

These values inserted into Equ. A2 lead to the non-dimensional form of the Navier-Stokes equations subjected to the Buossinesq approximation,

$$\frac{\partial \boldsymbol{u}^*}{\partial t^*} + (\boldsymbol{u}^* \cdot \nabla^*)\boldsymbol{u}^* + \nabla^* p^* - \mathrm{Re}^{-1} 2\mathbf{div}^*(\bar{\bar{\varepsilon}}^*(\boldsymbol{u}^*)) = -\mathrm{Fr}\,\boldsymbol{e}_z + (T^* - T_0^*)\,\frac{\mathrm{Gr}}{\mathrm{Re}^2}\boldsymbol{e}_z. \tag{A4}$$

If we now insert the following orders of magnitude that apply to our simulation problem,

$$\begin{aligned} &L = 1000\,\mathrm{m}, \quad U = 100\,\mathrm{m\,s^{-1}}, \quad \Delta T = 10\,\mathrm{K}, \\ &\beta = 10^{-3}\,\mathrm{K^{-1}}, \quad g = 10\,\mathrm{m\,s^{-2}}, \quad \mu = 10^{-5}\,\mathrm{Pa\,s^{-1}}, \quad \rho = 1\,\mathrm{kg\,m^{-3}}, \end{aligned} \tag{A5}$$

we obtain the following order for the non dimensional groups

$$\begin{aligned} \mathrm{Re}^{-1} &= \frac{\mu}{\rho U L} = \mathcal{O}(10^{-10}), \\ \mathrm{Fr}^2 &= g\,L\,U^{-2} = \mathcal{O}(1), \\ \frac{\mathrm{Gr}}{\mathrm{Re}^2} &= \beta \Delta T g L U^{-2} = \mathcal{O}(10^{-2}). \end{aligned} \tag{A6}$$

The small value of the inverse of the Reynolds-number, Re^{-1}, indicates negligibly small viscous- in relation to inertia forces, underlining the turbulent nature of the flow. The Froude-number, Fr, is of unity scale. This term, which is included in our equations, does not contribute to the dynamics of the flow, but only induces a hydrostatic pressure component. The non-dimensional group, $\mathrm{Gr}\,\mathrm{Re}^{-2}$, being smaller than unity indicates that inertia – on the

length scales we are interested in – dominates buoyancy. It is important to stress the fact that as soon as we either look at larger length scales and/or initially small velocities, corresponding to a complete study of katabatic winds starting from the interior of the ice sheet, this non-dimensional group can take values significantly larger than unity. In other words, a study of the complete katabatic wind originating from the ice sheet is not feasible with an incompressible flow model, whereas the impact of an incoming jet – being dominated by its inertia – can be approximated by our approach that assumes constant density.

The Supplement related to this article is available online at doi:10.5194/tcd-0-1-2015-supplement.

Acknowledgements. Mikko Lyly (ABB, Finland), Juha Ruokolainen (CSC – IT Center for Science Ltd., Finland) and Peter Råback (CSC – IT Center for Science, Ltd. Finland) are thanked for their support and expertise help on solving CFD problems with Elmer. We express our gratitude to Carleen Tijm-Reijmer (IMAU, Utrecht University, Netherlands), who provided us with the AWS data presented in Sect. 2. We thank both reviewers and the editor for their comments that significantly helped to improve the quality of this article. T. Malm was supported by the European Science Foundation Project – SvalGlac. J.C. Moore, M. Schäfer and T. Zwinger have been supported by the Finnish academy project: dynamical evolution of Scharffenbergbotnen blue ice area since the Late Glacial Maximum. All simulations were performed on the supercomputers of CSC-IT Center for Science, Ltd..

References

Axelsen, S.L. and van Dop, H.: Large-Eddy Simulation of Katabatic Winds. Part1: Comparison with Observations, Acta Geophys., 57 (4), 803-836, doi:10.2478/s11600-009-0041-6, 2009.

Bazilevs, Y., Michler, C., Calo, V. M., and Hughes, T. J. R.: Turbulence without Tears: Residual-Based VMS, Weak Boundary Conditions, and Isogeometric Analysis of Wall-Bounded Flows, ICES Report No. 08-07, Institute for Computational Engineering and Sciences, The University of Texas at Austin, Austin, 2008.

Bintanja, R.: On the glaciological, meteorological, and climatological significance of Antarctic blue ice areas, Rev. Geophys., 37, 337–359, doi:10.1029/1999RG900007,1999.

Bintanja, R. and Reijmer, C. H.: Meteorological conditions over Antarctic blue-ice areas and their influence on the local surface mass balance, J. Glaciol., 47, 37–50, 2001.

Bromwich, D. H., Du, Y., and Parish, T. H.: Numerical simulation of winter katabatic winds from west Antarctica crossing Siple Coast and the Ross Ice Shelf, Mon. Weather Rev., 122, 1417–1435, 1994.

Gallée, H.: Simulation of blowing snow over the Antarctic ice sheet, Ann. Glaciol., 26, 203–206, 1998.

Gallée, H. and Schayes, G.: Development of a three-dimensional meso-y primitive equation model: katabatic winds simulation in the area of Terra Nova Bay, Antarctica, Mon. Weather Rev., 122, 671–685, 1994

Geuzaine, C. and Remacle, J.-F.: Gmsh: a three-dimensional finite element mesh generator with built-in pre- and post-processing facilities, Int. J. Numer. Meth. Eng., 79, 1309–1331, 2009.

Giaever, J.: The White Desert: The official account of the Norwegian–British–Swedish Antarctic Expedition, Greenwood Pub Group, New York, ISBN 0-8371-1318-0, 1969

Gravemeier, V.: The Variational Multiscale Method for Laminar and Turbulent Incompressible Flow, Ph.D. thesis, Institut für Baustatik, Universität Stuttgart, Stuttgart, Bericht No. 40, ISBN 3-00-013034-9, 2003.

Gravemeier, V., Lenz, S., and Wall, W. A.: Variational multiscale methods for incompressible flows, in: International Conference on Boundary and Interior Layers, BAIL 2006, edited by: Lube, G. and Rapin. G., 24–28 July 2006, Göttingen, Germany, 2006.

John, V., Kindl, A., and Suciu, C.: Finite element LES and VMS methods on tetrahedral meshes, J. Comput. Appl. Math., 233, 3095–3102, doi:10.1016/j.cam.2009.06.005, 2010.

Kelley, C. T.: Iterative methods for linear and nonlinear equations, in: Frontiers in applies mathematics, SIAM, Philadelphia, 33–36, ISBN 0-89871-352-8, 1995.

Hättestrand, C. and Johansen, N.: Supraglacial moraines in Scharffenbergbotnen, Heimefrontfjella, Dronning Maud Land, Antarctica – significance for reconstructing former blue ice areas. Antarct Sci., 17, 225–236, doi:10.1017/S0954102005002634, 2005.

Hoffman, J. and Johnson, C.: A new approach to computational turbulence modeling, Comput. Methods Appl. Mech. Engrg., 195, 2865–2880,doi:10.1016/j.cma.2004.09.015, 2006.

Hoffman, J. and Johnson, C.: Computational Turbulent Incompressible Flow, Applied Mathematics: Body and Soul, 4, Springer, Berlin, Heidelberg, New York, doi:10.1007/978-3-540-46533-1, 2007.

Hughes, T. J. R.: Multiscale phenomena: Green's functions, the Dirichlet-to-Neumann formulation, subgrid scale models, bubbles and the origins of stabilized methods, Comput. Method. Appl. M., 127, 387–401, doi:10.1016/0045-7825(95)00844-9, 1995

Malm, T.: Simulation of Wind Fields at Scharffenbergbotnen, Antarctica and their Impact on Blue Ice Areas, M.S. thesis, Aalto University, School of Engineering, Espoo, Finland, available at: http://urn.fi/URN:NBN:fi:aalto-201207022723, 2012.

Moore, J. C., Nishio, F., Fujita, S., Narita, H., Pasteur, E., Grinsted, A., Sinisalo, A., and Maeno, N.: Interpreting ancient ice in a shallow ice core from the South Yamato (Antarctica) blue ice area using flow modeling and compositional matching to deep ice cores, J. Geophys. Res., 111, D16302, doi:10.1029/2005JD006343, 2006

Näslund, J. O., Fastook, J. L., and Holmlund, P.: Numerical modeling of the ice sheet in western Dronning Maud Land, East Antarctica: impacts of present, past and future climates, J. Glaciol. 46, 54–66, 2000.

Rautaheimo, P.: Developments in Turbulent Modelling with Reynolds-Averaged Navier-Stokes Equations, Ph.D. thesis, Helsinki University of Technology, Department of Mechanical Engineering, Espoo, Finland, ISBN 951-666-569-1, available at: http://urn.fi/urn:nbn:fi:tkk-002766, 2001.

Sinisalo, A.: Geophysical Exploration of Antarctic Blue Ice Areas (BIAs) for Paleoclimate Applications, Ph.D. Thesis, University of Oulu, Oulu, Finland, 2007.

Sinisalo, A. and Moore, J. C.: Antarctic Blue Ice Areas (BIAs) – towards extracting paleoclimate information, Antarct. Sci., 22, 99–115, doi:10.1017/S0954102009990691, 2010.

Sinisalo, A., Grinsted, A., and Moore, J. C.: Scharffenbergbotnen (Dronning Maud Land, Antarctica) blue-ice area dynamics, Ann. Glaciol., 39, 417–422, 2004.

Skyllingstad, E. D.: Large-eddy simulation of katabatic flows, Bound.-Lay. Meteorol., 106, 217–243, 2003.

Van den Broeke, M. R., Reijmer, C. H., van As, D., van de Wal, R. S. W., and Oerlemans, J.: Seasonal cycles of Antarctic surface energy balance from automatic weather stations, Ann. Glaciol., 41, 131–139, 2005.

Yu, Y. and Cai, X.: King, J. C., and Renfrew, I. A.: Numerical simulations of katabatic jumps in Coats Land, Antarctica, Bound.-Lay. Meteorol., 114, 413–437, 2005.

Zwinger, T., Schäfer, M., Martín, C., and Moore, J. C.: Influence of anisotropy on velocity and age distribution at Scharffenbergbotnen blue ice area, The Cryosphere, 8, 607–621, doi:10.5194/tc-8-607-2014, 2014.

Table 1. Physical parameter values used in the simulations. Fluid parameters were obtained for dry air at standard atmospheric pressure for a temperature of 243.15 K

Property	Symbol	Value	Unit
Density	ρ	1.45	$\mathrm{kg\,m^{-3}}$
Acceleration by gravity	$\boldsymbol{f} = -g\boldsymbol{e}_z$	9.81	$\mathrm{m\,s^{-2}}$
Dynamic Viscosity	η	1.57×10^{-5}	Pa s

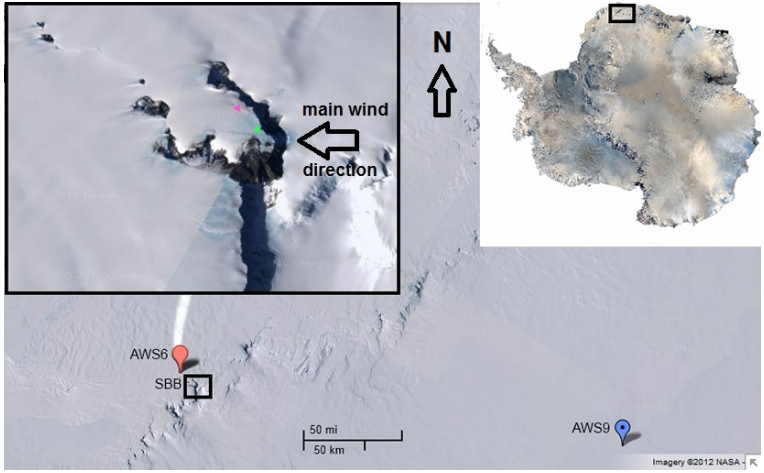

Figure 1. A map of Antarctica is shown at the top right with the domain shown in main image in the boxed area. In the main image, the AWS6 and AWS9 locations are marked and the Scharffenbergbotnen area is enclosed by the box and shown in detail at the top left. Windtails can be seen generally in a westerly direction from the nunataks, indicating winds from the east. The green triangle on the east border of the larger inner BIA shows where a field camp was located before it was destroyed by a storm on the 2–3 January 2007, and the magenta triangle shows where one destroyed tent was found after the storm with debris scattered over a wide area of the snow covered ground. Imagery courtesy of NASA.

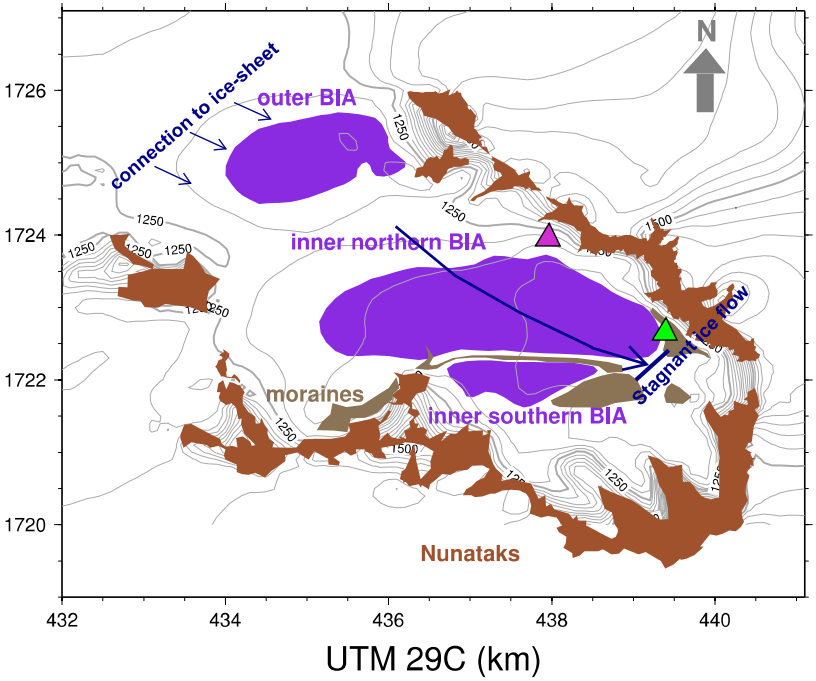

Figure 2. The Scharffenbergbotnen area, with the location of the Blue Ice Areas (purple), exposed rocks on top of hills and mountains (brown) and moraines (gray). Iso-lines of elevation are given in steps of 25 m. The inner BIAs are divided by a moraine into a northern and a southern BIA. Many of the other marked moraines are actually blue ice covered by rocks and much of the flatter area south and east of the inner blue ice areas is likely blue ice more or less covered by a thin layer of rocky material carried by ice flow from snow accumulation regions on the valley sides. Zwinger et al. (2014) show that ice flow to the inner northern BIA originates from snow accumulated on the ridge between it and the outer BIA, indicated by the long arrow in the figure. The green and magenta triangles represent the destroyed camp and loacation of debris (as in Fig. 1). Coordinates are in UTM 29 C system.

Figure 3. View over the northern inner BIA from the camp (marked with green triangle in Fig 1) looking towards the northwest, showing the destruction after the storm of the 2–3 January 2007. The arrow shows the location where the destroyed tent from the camp was found (magenta triangle in Figs. 1 and 2). The photo was taken by J.C. Moore.

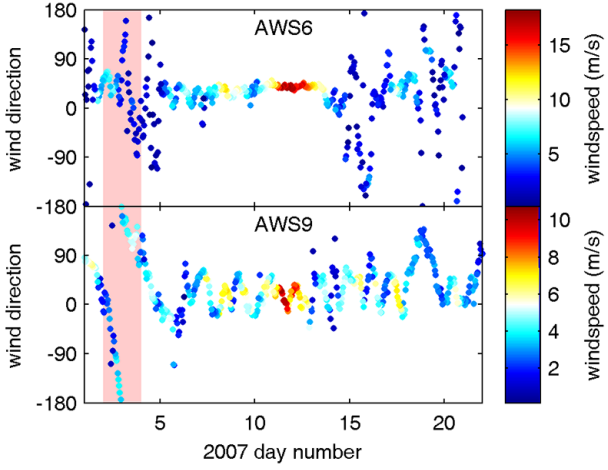

Figure 4. Wind speed and direction of automatic weather stations AWS6 and AWS9 (see Fig. 1 for their position) for the first 22 days of 2007. The storm event that destroyed the camp (Fig. 3) was during the pink shaded period, when winds were low at both AWSs. A synoptic storm occurred around 12 January, when conditions in the SBB valley were calm.

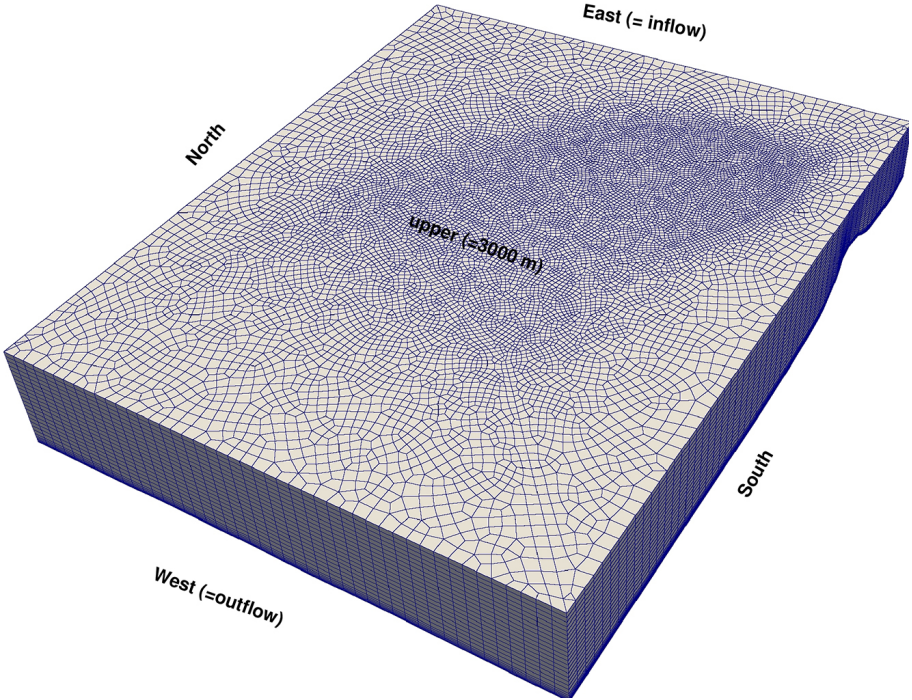

Figure 5. The discretized domain, Ω. Horizontal resolutions reach from 50 m close to the valley slopes to 200 m. The vertical terrain following extrusion is not equidistant, but rather features a mesh refinement in the lower 10 % of the height in order to capture boundary layer effects.

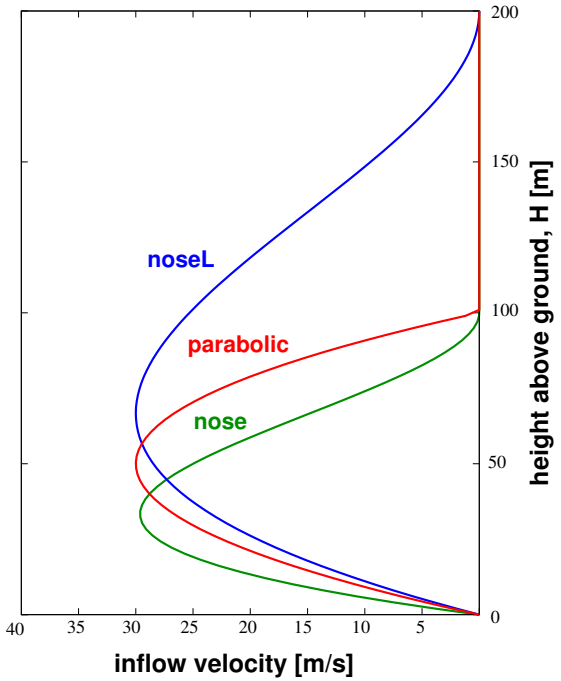

Figure 6. Normal inflow velocities at the eastern boundary, resembling the katabatic wind front.

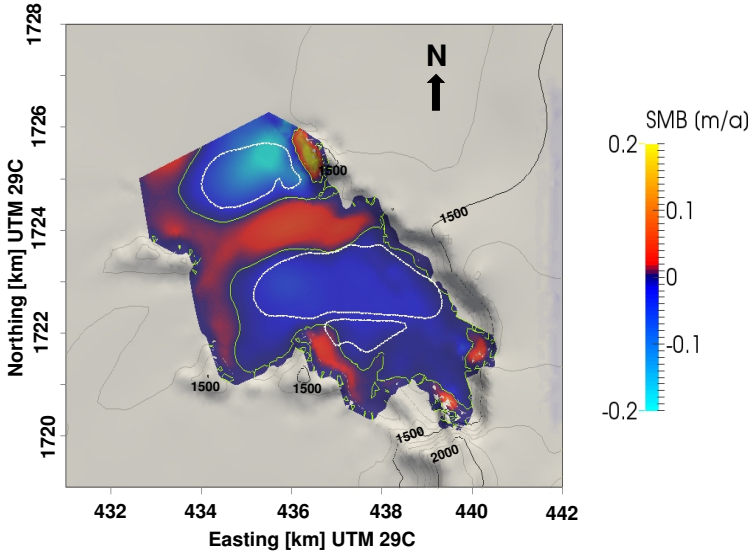

Figure 7. The computed equilibrium surface mass balance from the ice flow simulation by Zwinger et al. (2014). The colours – confined to the glaciated area inside the valley – show the equilibrium surface mass balance (Eq. 10) in $\mathrm{m\,a^{-1}}$ ice equivalent (density of ice, $\rho_i = 910\,\mathrm{kg\,m^{-3}}$). The yellow line confines the ablation zones and the white lines depict the outline of the BIAs (see Fig. 2). The gray contour lines show the elevation of the wider terrain in steps of 100 m, the black in steps of 500 m (annotated by their values).

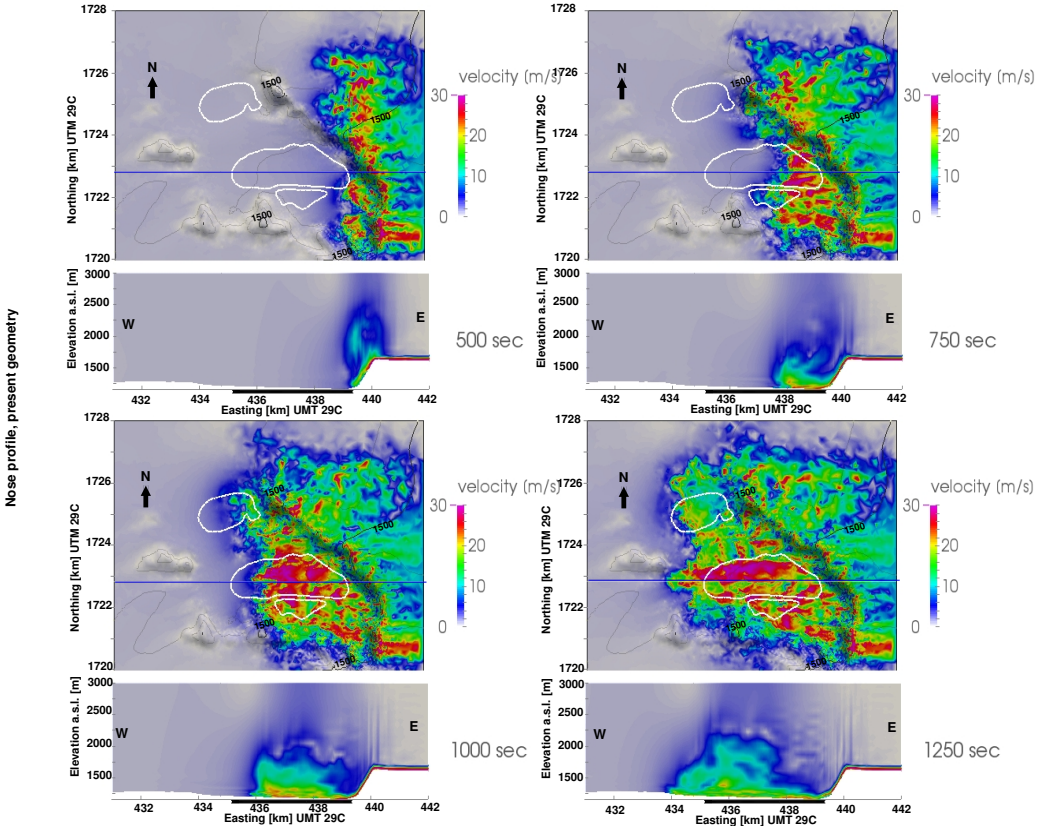

Figure 8. Velocity magnitude 5 m above the surface and in a vertical cross-section from east to west through the valley (marked by the horizontal blue line in plan views). Results from the simulation using the nose profile (Eq. 5) displayed at 500, 750, 1000 and 1250 s into the simulation. The white lines in the plan-views and the black bar under the cross-sections denote the positions of the BIAs. The cross-sections are stretched vertically by a factor of two. The velocity scale is truncated at 30 $m\,s^{-1}$.

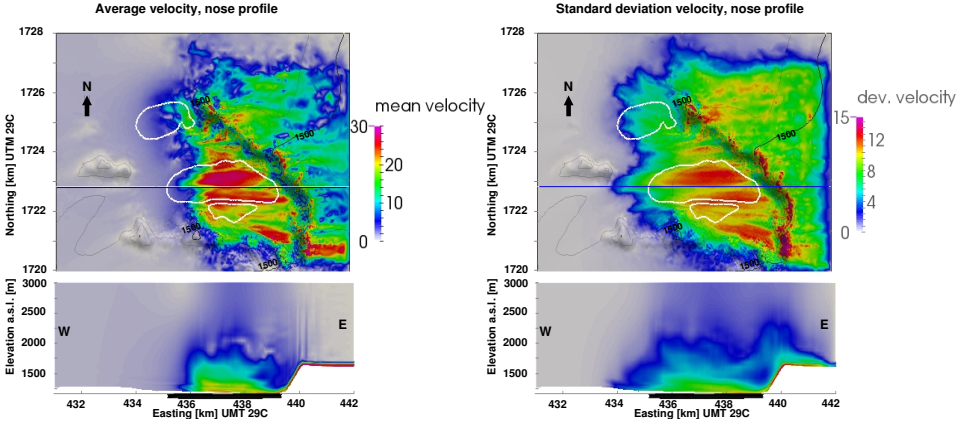

Figure 9. Statistics performed on the simulation using the nose profile (Eq. 5) using results from 950 - 1050 s (in steps of 5 s). The left panel shows the averaged velocity magnitude 5 m above the surface and in a vertical cross-section from east to west through the valley (marked by the horizontal blue line in plan views). The velocity scale is truncated at 30 m s^{-1}. The right panel shows the standard deviation from the average value of the velocity magnitude, which stands for a measure on the large scale turbulence of the flow. This scale is truncated at 15 m s^{-1}. The cross-sections are stretched vertically by a factor of two.

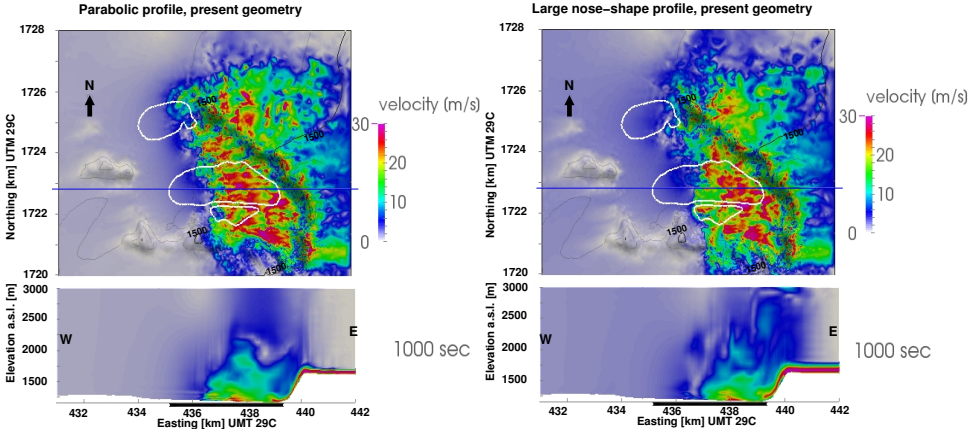

Figure 10. Velocity magnitude 5 m above the surface and in a vertical cross-section from east to west through the valley (marked by the horizontal blue line in plan views) of the simulations using the parabolic (Eq. 6) and the upscaled nose profile (Eq. 7) displayed at 1000 s into the simulation. The white lines in the plan-views and the black bar under the cross-sections denote the positions of the BIAs. The cross-sections are stretched vertically by a factor of two. The velocity scales are truncated at 30 m s^{-1}.

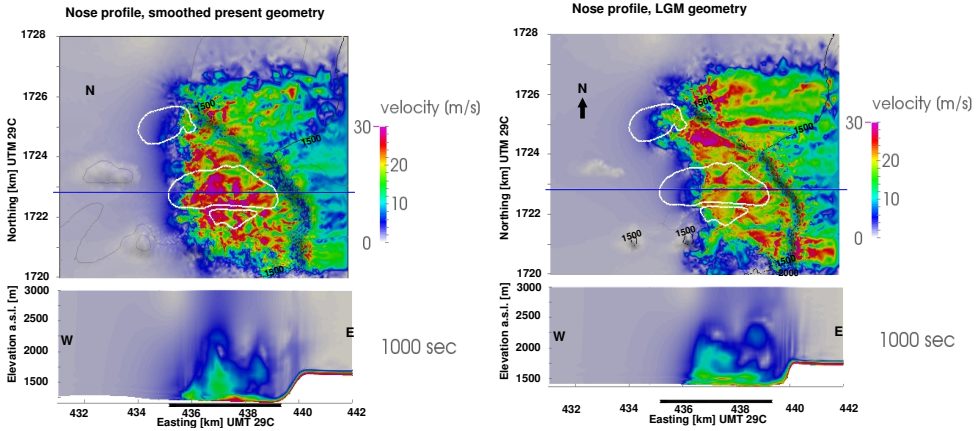

Figure 11. Velocity magnitude 5 m above the surface and in a vertical cross-section from east to west through the valley (marked by the horizontal blue line in plan views) of the simulation using the nose-shape (Eq. 5) profile on a smoothed present day terrain (left) and on the LGM terrain (right) displayed at 1000 s into the simulation. The white lines in the plan-view and the black bar under the cross-section denote the positions of the BIAs. The cross-sections are stretched vertically by a factor of two. The velocity scales are truncated at 30 m s^{-1}.